HHS Public Access

Author manuscript

J Vis Exp. Author manuscript; available in PMC 2021 January 28.

Using the Chicken Chorioallantoic Membrane In Vivo Model to Study Gynecological and Urological Cancers

Allison C. Sharrow[1], **Moe Ishihara**[1], **Junhui Hu**[1], **Il Hyun Kim**[1], **Lily Wu**[1]

[1]Molecular and Medical Pharmacology, University of California Los Angeles

Abstract

Mouse models are the benchmark tests for in vivo cancer studies. However, cost, time, and ethical considerations have led to calls for alternative in vivo cancer models. The chicken chorioallantoic membrane (CAM) model provides an inexpensive, rapid alternative that permits direct visualization of tumor development and is suitable for in vivo imaging. As such, we sought to develop an optimized protocol for engrafting gynecological and urological tumors into this model, which we present here. Approximately 7 days postfertilization, the air cell is moved to the vascularized side of the egg, where an opening is created in the shell. Tumors from murine and human cell lines and primary tissues can then be engrafted. These are typically seeded in a mixture of extracellular matrix and medium to avoid cellular dispersal and provide nutrient support until the cells recruit a vascular supply. Tumors may then grow for up to an additional 14 days prior to the eggs hatching. By implanting cells stably transduced with firefly luciferase, bioluminescence imaging can be used for the sensitive detection of tumor growth on the membrane and cancer cell spread throughout the embryo. This model can potentially be used to study tumorigenicity, invasion, metastasis, and therapeutic effectiveness. The chicken CAM model requires significantly less time and financial resources compared to traditional murine models. Because the eggs are immunocompromised and immune tolerant, tissues from any organism can potentially be implanted without costly transgenic animals (e.g., mice) required for implantation of human tissues. However, many of the advantages of this model could potentially also be limitations, including the short tumor generation time and immunocompromised/immune tolerant status. Additionally, although all tumor types presented here engraft in the chicken chorioallantoic membrane model, they do so with varying degrees of tumor growth.

Keywords

chicken chorioallantoic membrane; CAM; disease models; animal; heterografts; patient-derived xenograft; transplantation; heterotopic; ovarian neoplasms; urologic neoplasms; in ovo

Correspondence to: Allison C. Sharrow at asharrow@mednet.ucla.edu, Lily Wu at LWu@mednet.ucla.edu.

Disclosures

The authors have nothing to disclose.

Video Link

The video component of this article can be found at https://www.jove.com/video/60651/

Introduction

Mice have served as the classic model organism for the study of human diseases, including malignancy. As mammals, they share many similarities with humans. Their high degree of genetic similarity has permitted transgenic manipulation of the mouse genome to provide enormous insight into the genetic control of human diseases[1]. Extensive experience in the handling of and experimentation with mice has resulted in their being the model of choice for biomedical research. However, in addition to the ethical and scientific concerns regarding murine models, they can also be quite costly and time consuming[2,3]. The development of tumors can take weeks or even months. The housing at a typical institution alone can run in the hundreds to thousands of dollars while tumors are developing. Ovarian cancer is an example of this drawback because its growth in murine models can easily take months. Delays in research progress potentially impact ovarian cancer patients' persistently low 5-year survival rate of only 47% (i.e., an increase in survival of only 10% over 30 years)[4]. Similarly, urological cancers (kidney, prostate, and bladder cancers) constitute 19% of all cancer cases in the United States and 11% of cancer-related deaths[4]. Thus, a novel in vivo approach to study gynecological and urological cancers could save a laboratory considerable time, labor, and money, even if this model is only applied to initial screening experiments. Additionally, the resulting acceleration of research findings could significantly impact the 177,000 individuals diagnosed with these cancers annually.

The chicken CAM model offers many advantages that address the aforementioned issues. A popular model to study angiogenesis[5,6], tumor cell invasion[7,8], and metastasis[7,9], the chick embryo CAM model has already been used to study many forms of cancers, including glioma[10,11,12], head and neck squamous cell carcinoma[13,14], leukemia[15,16], pancreatic cancer[17], and colorectal cancer[18]. Additionally, CAM models have been generated for neuroblastoma[19], Burkitt lymphoma[20], melanoma[21], and feline fibrosarcoma[22]. Prior studies have also presented engraftment of bladder cancer[23] and prostate cancer cell lines[24], but with limited protocol details. Not only are eggs much cheaper than mice, but they also produce highly reproducible results[25,26]. They show fast vasculature development, and tumor engraftment can occur in as quickly as a few days and be visualized longitudinally through the open window. With the 21 day time frame between egg fertilization and hatching, experiments can be completed within a few weeks. Furthermore, the low cost, limited housing needs, and small size readily permit large-scale experiments that would be prohibitive for mouse studies.

Therefore, we sought to optimize the CAM model for the engraftment of gynecological and urological cancers. Due to the immunocompromised status of the early chicken embryo[27], both mouse and human cells can be readily implanted. As such, we have successfully engrafted ovarian, kidney, prostate, and bladder cancers. For each of these tumor types, the CAM readily accepts established murine and/or human tumor cell lines. Importantly, freshly harvested primary human tumor tissues can also engraft from either digested cells or pieces of solid tissue with high rates of success. Each of these cancer types and cell sources requires optimization, which we share here.

Protocol

All of the experiments presented herein were reviewed and approved by the appropriate ethical committees at the University of California, Los Angeles (UCLA). The use of deidentified, primary human tumors has been approved by the UCLA Institutional Review Board (Protocol numbers 17–000037, 17–001169, and 11–001363). At UCLA, Animal Research Committee review is not required for experiments using chicken embryos; protocol approval is only required when the eggs will be hatched. However, best practices, such as the AVMA Guidelines for the Euthanasia of Animals, were used to handle chicken embryos ethically and to avoid pain as much as possible. Researchers are urged to verify the oversight requirements at their institution prior to initiating studies using CAM models.

1. Preparing the eggs

1. Before receiving the eggs, assemble and equilibrate the egg incubator to 37.8 °C (100 °F) with 60–70% humidity following the manufacturer's instructions.

   NOTE: To minimize contamination risks, autoclaved water may be used to control the humidity.

2. Upon receiving fertilized, Rhode Island Red chicken eggs from a certified laboratory-grade egg supplier, dry wipe the surface of the shells with paper towels. A lightly dampened paper towel may be used to remove adhered material. Dry immediately.

   NOTE: Wetting the shell with liquid below 43.3 °C can introduce bacteria into the egg. If one chooses to wash or disinfect the eggs, the temperature of the liquid must be between 43.3–48.9 °C. Higher temperatures can boil the eggs. The choice of disinfectant should be made based on the microorganisms causing concern.

3. Use a pencil or marker to label the date on the egg. This is considered development day 0.

4. Place the eggs into the egg incubator and incubate for at least 7 days with rotation to permit CAM development. An automatic rotator may be used, or the eggs may be rotated 180° 2–3x per day.

2. Opening the eggs

NOTE: Opening of the eggs should be done when the CAM has fully developed. This is typically on development day 7 or 8.

1. Disinfect a biosafety cabinet with 70% ethanol. Similarly disinfect and place into the biosafety cabinet an egg rack, egg candler, marker, cordless rotary tool with a silicon carbide grinding stone and circular cutting wheel, 18 G needle, pipet controller with quarter-inch vacuum tubing, packing tape, office scissors, curved scissors, Semken (or similar) forceps, cotton balls, and 6 × 7 cm transparent film dressing. Whenever possible, use sterile, disposable or autoclaved tools.

2. Turn off the egg rotator. Place approximately 1–3 eggs into the biosafety cabinet on the egg rack. While in the dark, place the egg candler against the eggshell to identify the air cell. Mark the location of the air cell.

   NOTE: The intensity of illumination from the egg candler is crucial for visualizing the interior of the egg. If the air cell or vasculature is consistently difficult to see, try replacing the egg candler batteries.

3. Move the egg candler over the shell to find a large blood vessel network. Rotate the egg if necessary. An ideal vasculature will be branching near the middle of the egg. Use a marker to draw over the vasculature to be used for implantation.

4. Turn on the light in the hood. Using a cordless rotary tool fitted with a silicon carbide grinding stone, drill a small hole in the shell directly over the center of the air cell. Drill until most of the shell has been removed, but the white, inner membrane is intact.

   NOTE: Drilling over the air cell before targeting the vasculature permits determining the thickness of that particular eggshell over the air cell rather than over the CAM and vasculature. If the CAM or vasculature is disrupted, then the egg is not useable for implantation.

5. Drill and open another small hole where the vascular window will be opened as was done for the air cell (step 2.4).

6. Using an 18 G needle, gently pierce through the white, inner membrane over the air cell and vasculature. If unable to penetrate the shell, then carefully drill a little more. Ensure that the white, inner membrane (but not the CAM) is disrupted throughout the entirety of the drilled area.

   Removal of the membrane piece is not necessary.

   NOTE: If the CAM or vasculature is disrupted during this step, discard the egg. Damage is evident if there is blood or albumin leaking from a drilled hole.

7. Turn off the hood light. Using the egg candler, verify that the air cell was transferred from the end of the egg to the area over the vasculature. If necessary, place the vacuum tubing inserted into a pipet controller around the hole over the original air cell and gently apply suction in short bursts to move the air cell.

8. Use a marker to outline the new location of the air cell approximately 0.5 cm inside the air-CAM boundary. Affix a piece of packing tape just over the new air cell. If necessary, use standard office scissors to trim the tape to an appropriate size.

   NOTE: Tape can disrupt airflow through the shell and should not be larger than necessary to fully cover the air cell.

9. Return the eggs to the incubator to warm without rotation with the new air cell facing up. Repeat steps 2.2–2.9 for the remaining eggs to be opened.

NOTE: The protocol may be paused here. If unsure of the quality of CAM development, a small number of eggs should proceed through step 2.16 prior to opening the remaining eggs.

10. Place approximately 1–3 eggs with relocated air cells onto the egg rack in the biosafety cabinet.

NOTE: Care should be taken to avoid introducing contamination into the opened egg. Therefore, always open eggs inside a biosafety cabinet, and use sterile tools and equipment whenever possible.

11. Using a cordless rotary tool fitted with a circular cutting wheel, cut a small line over the air cell boundary drawn in step 2.8. Ensure that this is approximately 0.5 cm inside the actual air-CAM boundary to avoid disrupting the CAM or vasculature. Cut completely through the shell but be careful not to penetrate deeply enough to disrupt the CAM or vasculature.

12. Using curved scissors, cut around the remaining air cell to create a window in the shell.

NOTE: If blood or membrane is present on the removed shell, then the egg is not suitable for implantation. If a high proportion of the eggs are not cleanly opened, consider waiting at least 1 additional day to open the remaining eggs to permit better CAM formation. If the shells of the remaining eggs have not been pierced, rotation of the eggs within the incubator should be resumed.

13. Verify the viability of the embryo. Viable embryos will display extensive vasculature, clear albumin, embryo movement, or a visible heartbeat.

14. Using Semken forceps, pull small pieces of cotton from a sterile cotton ball. Gently blot the CAM surface to remove the shell dust and debris.

NOTE: The removal of debris must be performed on the same day that the eggs are opened.

15. Cover the shell opening with a one-quarter piece of 6 × 7 cm transparent film dressing.

16. Return the eggs to the incubator. Ensure that the egg sits securely with the opened window facing up and the CAM not touching the transparent film dressing. Use a piece of egg rack, the edge of the egg rotator, or another suitable item to prop any eggs that keep rolling.

17. Repeat steps 2.10–2.16 for all remaining eggs to be opened.

NOTE: The opening of the eggs does not need to be completed on the same day as implantation. Waiting at least 1 day can help eliminate eggs whose viability was compromised by opening the shell.

3. Preparing the cancer cell suspension for transplantation (option 1)

NOTE: This is to be completed just prior to the implantation, which should ideally take place between days 7 and 10. Please see notes at the beginning of step 5 or 6 for further

information concerning the implantation date. This approach was used for all the cell lines and cultured kidney cancer tumor digests.

1. Thaw the extracellular matrix solution on ice.
2. Using mechanical and/or enzymatic digestion, obtain a single cell suspension using a method appropriate for the cell type being implanted.
3. Resuspend the total number of cells to be implanted in an appropriate medium for implantation. Implants of 1–2 × 10^6 cells per egg are typical.

   NOTE: The medium used for the implantation of the cell lines is typically the complete medium used for culturing the cells, containing FBS or serum replacement. The implantation of tumor digests typically uses the complete medium used for culturing cell lines of the same cancer type. However, adjustments to the medium formulation may be made if needed experimentally. The effects on tumor development and growth would need to be empirically determined.
4. Pellet the cells using a centrifuge speed and time appropriate for the cells being used. Typical speeds are 250–300 × *g*, and times are 5–10 min.
5. Remove the supernatant from the pelleted cells by pipetting. Mechanically resuspend the cells in the residual medium via flicking or pipetting. Place on ice to cool. Measure the volume of cells and medium using an appropriately sized pipet.
6. Calculate implantation volumes such that 1–2 × 10^6 cells are implanted in a volume of 20–100 μL per egg with a final extracellular matrix concentration of 2.7–4 mg/mL protein. Add medium, any desired growth factors or additives, and extracellular matrix solution according to this calculation. Keep on ice until ready to implant.

   NOTE: For the calculations in steps 3.3 and 3.6, an extra volume of at least one-half egg implant should be incorporated to ensure an adequate volume for all eggs in the group. For implantation of the ovarian cancer cell lines (i.e., SKOV3 and ID8), 10^6 cells per egg were implanted. For implantation of the renal cell carcinoma cell line RENCA, cultured cells derived from digested primary human renal cell carcinoma, prostate cancer cell lines (i.e., CWR, C4–2, and MyC-CaP), and bladder cancer cell lines (i.e., HT-1376 and T24), 2 × 10^6 cells were implanted.

4. Preparing tumor pieces for implantation (option 2)

NOTE: This is to be completed just prior to implantation, which should ideally take place between days 7 and 10. Please see notes at the beginning of step 5 or 6 for further information concerning the implantation date. Primary ovarian and bladder cancers were implanted as tumor pieces.

1. Thaw extracellular matrix solution on ice. Dilute to a final protein concentration of 2.7–4 mg/mL in an appropriate medium containing any desired growth factors or additives. Keep on ice.

   NOTE: Implantation of tumor pieces typically uses the complete medium used for culturing cell lines of the same cancer type. However, adjustments to the medium formulation may be done if needed experimentally. The effects on tumor engraftment and growth would need to be empirically determined.

2. Using a scalpel or scissors, excise pieces from the fresh tumor. Ideal sizes range from 2–5 mm on each side. Keep tissues immersed in the medium until ready to implant.

5. Implantation using a nonstick ring (option 1)

NOTE: Cells may be implanted beginning on development day 7 if the CAM is fully developed. Implantation can occur any time prior to hatching that permits adequate time for tumor development and the desired experiment, but note that the embryo's immune cells begin to be present around day 10 postfertilization[27]. Tumor growth rate varies considerably by cell type and needs to be empirically determined for the cell type of interest. The ovarian cancer and the prostate cancer cells were implanted using the nonstick ring method. Note that when a nonstick ring is not available, a pipet tip may be cut to a similar size and used.

1. Use 70% ethanol to disinfect a biosafety cabinet and all the required tools: an egg rack, curved iris forceps, nonstick rings (1/4 inch inner diameter), glass stir rod, appropriate volume pipets and tips, 6 × 7 cm transparent film dressing, office scissors, and marker or pencil. Whenever possible, sterile, disposable or autoclaved tools should be used.

2. Place eggs to be implanted on an egg rack in a biosafety cabinet. Select a manageable number of eggs. Up to six is typical. Avoid allowing the eggs to cool substantially while working with them.

3. Remove transparent film dressing from the shell by rolling the edges towards the open window to avoid pulling away pieces of shell. Check that the eggs are viable and healthy. Ideal eggs will have a large vessel in the center of the opened area with smaller vessels branching from it.

4. Using curved iris forceps, place a sterile, nonstick ring onto the CAM over the vessel, ideally over a branch point. Use a sterile glass stir rod to gently abrade the CAM.

5. Pipet the cell suspension from step 3.6 into the center of the nonstick ring. Alternatively, use forceps to place a tumor piece from step 4.2 into the center of the nonstick ring and cover with 20–50 μL of the extracellular matrix solution generated in step 4.1.

6. Seal the opening with a one-quarter piece of 6 × 7 cm transparent film dressing. Label the eggs with an appropriate implant designation.

   NOTE: Numbering the eggs within a group facilitates longitudinal observations.

7. Return the egg to the incubator. Ensure that the opening of the shell sits upright and that the egg is secure.

   NOTE: Eggs can be returned to an egg incubator without rotation. Alternatively, high postimplant viability can be obtained using a 37–38 °C cell incubator with the CO_2 deactivated and a hygrometer to monitor the humidity, which should be 50%−80%.

6. Implantation without a nonstick ring (option 2)

NOTE: Cells may be implanted beginning on development day 7 if the CAM is fully developed. Implantation can occur any time prior to hatching that permits adequate time for tumor development and the desired experiment, but note that the embryo's immune cells begin to be present around day 10 postfertilization[27]. This method was used for implanting the renal cell carcinoma cells and the bladder cancer cells.

1. Use 70% ethanol to disinfect a biosafety cabinet and all required tools: appropriate volume pipets and tips, sterile 10-cm tissue culture dishes, egg rack, 6 × 7 cm transparent film dressing, office scissors, and marker.
2. Aspirate an inoculation volume of the cell suspension generated in step 3.6 into an appropriately sized pipet tip (200 µL is typical). While holding the top portion of the tip, carefully eject the pipet tip and place horizontally into a sterile, 10-cm tissue culture dish.
3. Repeat step 6.2 for all samples within a group with one dish for each group.
4. Place tips into a 37 °C incubator for 15–30 min to allow the extracellular matrix to partially polymerize.
5. After 15 min of incubation, begin checking for polymerization. A small amount of liquid typically leaks out of the tip when placed onto the dish. Polymerization of this liquid can be used to estimate the extent of polymerization of the liquid within the tip.
6. Place the eggs to be implanted on an egg rack in a biosafety cabinet. Select a manageable number of eggs. Up to six is typical. Avoid allowing the eggs to cool substantially while working with them.
7. Remove the transparent film dressing from the shell by rolling the edges towards the open window. This avoids pulling away pieces of shell.
8. Check that the eggs are viable and healthy. Ideal eggs will have a large vessel in the center of the opened area with smaller vessels branching from it.
9. Place one pipet tip onto an appropriately sized pipet. Depress the plunger to force the partially polymerized cell suspension onto the CAM over a large, well-developed vessel, ideally over a branch point.
10. Seal the opening with a one-quarter piece of 6 × 7 cm transparent film dressing.
11. Label the egg with an appropriate implant designation.

NOTE: Numbering the eggs within a group facilitates longitudinal observations.

12. Return the egg to the incubator. Ensure that the opening of the shell sits upright and that the egg is secure.

    NOTE: Eggs can be returned to a dedicated egg incubator without rotation. Alternatively, high postimplant viability can be obtained using a 37–38 °C cell incubator with the CO_2 deactivated and a hygrometer to monitor the humidity, which should be 50%−80%.

7. Bioluminescence imaging of firefly luciferase marked tumors

NOTE: If the implanted cells were stably transduced with the gene encoding firefly luciferase or other imaging factors, then the resulting tumors may be visualized using bioluminescence imaging. Fluorescence imaging is not recommended on intact eggs due to high background from the eggshell. This is endpoint analysis, as the opening of the shell drastically reduces survival. Tumors may be imaged at any time that is appropriate for experimental needs and the speed of tumor growth. However, on average, eggs hatch 21 days postfertilization. Therefore, development day 18 is an appropriate endpoint to avoid unwanted hatching.

1. If necessary, transport eggs to the imaging facility. Tape eggs onto 10-cm tissue culture dishes. Return them to a 37.8 °C (100 °F) egg incubator with the rotation mechanism removed or deactivated. Humidity is not crucial for transport and imaging.

2. Using curved iris forceps, gently push the CAM away from the shell until the CAM is flush with the albumin and embryo. Using wide-tipped specimen forceps, break away pieces of the shell to expand the shell opening adequately for tumor visualization.

3. Inject a minimum of 50 μL of 30 mg/mL D-luciferin into the egg albumin. A similar volume of D-luciferin may also be pipetted into the nonstick ring or onto the surface of the CAM in the area containing the implanted cells. This ensures optimal bioluminescence in the absence of an ideal vascular supply. Incubate for 8 min.

4. Inject 20–50 μL of isoflurane into the albumin of the egg to anesthetize the egg. Incubate for an additional 2 min. Alternatively, the egg may be placed into an induction chamber containing 2–2.5% vaporized isoflurane. Adequate anesthesia depth is obtained when embryonic movement ceases.

   NOTE: Larger volumes of isoflurane (100 μL) can be used to euthanize the egg.

5. Place eggs into a bioluminescence imaging device and image using appropriate settings as determined by the manufacturer’s instructions.

   For this study, an exposure time of 1 min was used.

6. To image the remaining CAM and embryo, open the egg into a 10-cm tissue culture dish.

1. Grasp the egg with the fingers of both hands on the underside of the egg near the middle of the egg and the thumbs on either side of the shell opening.
2. Gently pull apart the two halves of the egg with the thumbs while gently pressing into the egg with the fingers.
3. When the shell is approximately half-separated from the CAM and embryo, flip the egg upside down over a 10-cm tissue culture dish.
4. Continue to separate the shell halves. If the CAM sticks to the inside of the shell, gently use the fingers to push the CAM away from the shell.
5. The embryo may be flipped into another dish if desired.
6. If necessary, additional isoflurane may be administered as in step 7.4.

8. Tumor harvesting

NOTE: Tumors may be harvested at any time that is appropriate for the experimental needs and the speed of tumor growth. However, on average, eggs hatch 21 days postfertilization. Therefore, development day 18 is an appropriate endpoint to avoid unwanted hatching.

1. Grasp tumor with forceps. Using scissors (spring iris scissors work well) or a scalpel, carefully excise tumor from CAM.
2. If the tumor has been transduced with the firefly luciferase gene, reimaging may be performed to verify successful removal of difficult-to-visualize tumors.

   NOTE: Excised tumors may be analyzed by any method appropriate for a particular experiment. Tumors may also be reimplanted into CAM or mice. To confirm tumor identity, tumors may be fixed, paraffin embedded, and examined with hematoxylin and eosin or immunohistochemical staining.

Representative Results

Thus far, we have found this method of implantation to be successful for ovarian, kidney, prostate, and bladder cancers. Each was optimized to identify specific conditions for implantation, although there may be flexibility. Of the tested tumor types, ovarian cancer growth was much less pronounced and typically not visible without the assistance of bioluminescence imaging (Figure 1). However, a stiffening of the CAM could be felt with forceps in the area of implantation. This may help identify possible tumor growth in the absence of bioluminescence imaging, though further validation would be required via histology or another suitable method. We achieved successful engraftment of both human and murine cell lines that show morphologies consistent with those seen in other in vivo models (Figure 1A and 1B). In addition, the implantation of tumor pieces was possible (Figure 1C, blue arrow indicates tumor). The implanted tumor in this case came from a patient with high-grade, metastatic, ovarian serous carcinoma. The resulting tumors morphologically resembled their tumors of origin and expressed human-specific proteins, such as cytokeratin 8/18, that readily permit their differentiation from CAM and chicken embryonic tissues.

When optimizing tumor engraftment and growth, appropriate growth factors or hormones may be added at the time of implantation. For example, a subtle, nonsignificant increase in tumor size (as measured by total radiance flux) was observed in ID8 cells when supplemented with three units (U) of human follicle stimulating hormone (FSH) at the time of implantation (Figure 1D). The selection of FSH for ovarian cancer growth stemmed from the expression of the FSH receptor in ID8 cells and the high levels of FSH typically found in postmenopausal women, who constitute the majority of ovarian cancer cases. Similar approaches may be adopted for other difficult-to-grow cancer types to enhance the utility of the CAM model. Furthermore, FSH was only added at the time of cell implantation. Replenishing the growth factor or hormone could be accomplished by pipetting an appropriate amount of the additive in the medium into the nonstick ring at appropriate intervals, which could enhance the effect.

For kidney cancer, implantation of 2×10^6 clear cell renal cell carcinoma cells from established cell lines, such as RENCA, produced rapid, robust tumor formation, though lower cell doses may also be used (Figure 2A, 10 days postimplantation). Resulting tumors morphologically resembled those obtained through standard mouse in vivo models[28]. Implantation of RENCA cells marked with firefly luciferase permitted bioluminescence imaging. Primary human tumors may also be implanted. The pieces of tumor persisted and recruited vasculature without showing significant growth. Implantation of digested cells originating from a primary, clear cell renal cell carcinoma that were expanded in vitro, however, grew similarly to the established cell lines (Figure 2B). Renal cell carcinoma cells may be seeded using either the nonstick ring method or the method without the nonstick ring.

Multiple human and murine prostate cancer cell lines were tested for CAM engraftment (Figure 3). Each grew well when 2×10^6 cells were implanted using the nonstick ring. Histological evaluation of the resulting tumors was consistent with expectations for each cell line. Additionally, implantation of cells stably marked with firefly luciferase permitted tumor identification with bioluminescence imaging (Figure 3A).

Bladder cancer was established in the CAM model from established cell lines and pieces of primary human tissue (Figure 4). Cell lines grew well when implanted with 2×10^6 cells without the nonstick ring (Figure 4A and 4B), although implantation with the ring was successful. Primary human tumor may be implanted from pieces of tissue (Figure 4C). The presented case originated from a patient with high grade, non-muscle-invasive, urothelial carcinoma. Implantation of digested cells has not yet been attempted due to ongoing tumor digestion optimization. Cancer cells of the resulting CAM tumors retained the morphology of the original tumor, but with an altered stromal component. Tumor growth was less than for renal cell carcinoma and prostate cancer, though still readily visible.

To ensure a high number of viable, assayable eggs at the endpoint, care must be taken when incubating and opening the eggs. If the incubator conditions are suboptimal either before or after implantation, then embryo viability may be compromised. If significant embryonic death occurs, troubleshoot the incubator conditions according to the manufacturer’s instructions. In our experience, temperature and humidity stability appear to be more crucial

than their exact values. Therefore, we found that incubating the inoculated eggs in a modified, cell-culture, CO_2 incubator achieved superior viability over retaining the eggs in small, dedicated egg incubators that require more frequent opening to replenish the water that controls the humidity. Minimizing the frequency with which the inoculated eggs are removed for tumor examination may also enhance embryo viability.

An additional concern of CAM implantation is the integrity of the CAM at inoculation. If the CAM is not intact after opening the shell, then the nonstick ring and implanted cells will sink into the albumin of the embryo (see the note after step 2.12). This causes cancer cell dispersal. Some tumors may still form, but cancers that receive significant growth and survival signaling from neighboring cancer cells, such as ovarian cancer, will not reliably form tumors under such conditions. If nonstick rings are used for implantation, the failure of the CAM can be identified by the sinking of the ring into the albumin. This must be distinguished from cases in which the ring and implanted cells were moved to the bottom of the egg by embryonic movement. In those cases, the ring will be found between the CAM and the underside of the shell. Embryonic movement cannot be controlled. However, ring placement can make it more difficult for the embryo to disrupt the implanted cells. Rings placed at the edges of the air pocket generated in step 2.7 are more likely to be moved by the embryo than those placed at the center of the field.

Discussion

Tumor expansion and engraftment using the CAM model permits more rapid and directly observable tumor growth than existing in vivo animal models. In addition, costs are significantly lower once the initial purchase of equipment is complete, especially when compared to the cost of immunocompromised mice. The initial, immunocompromised state of chicken embryos readily permits engraftment of human and murine tissue. Even with these strengths, the CAM model does have limitations. The short time that can be a benefit could also be a detriment if long-term treatment studies are warranted. The immunocompromised/immune tolerant status of the CAM model could complicate studies of tumor-immune interactions. For these studies, coimplantation of immune cells of interest may be necessary, possibly with replenishment of the immune compartment. Furthermore, although all the tumor types we presented engraft into the CAM model, they do so with varying degrees of growth. For example, renal cell carcinoma rapidly forms large tumors, but ovarian cancer tumors are difficult to visualize without the assistance of bioluminescence imaging. Tumor growth and speed would need to be assessed for a particular tumor type to determine if the CAM would be a suitable experimental model.

Successful tumor engraftment requires the careful completion of specific steps of the protocol. First, eggs need to be incubated under ideal conditions to have optimal embryo survival and CAM formation prior to engraftment. Due to the natural variability in batches, we suggest obtaining excess eggs from the specific egg supplier. We have also found that cooler, rainier weather can lead to fungal growth in the eggs. During wetter weather, more eggs may need to be engrafted to obtain adequate yields at the endpoint. This seasonal variation is likely to be region-specific. Adequate CAM formation is essential for successful tumor engraftment. Any indications of the CAM remaining attached to the shell when

opening should not be ignored. If several eggs fail to have intact CAM when opening the first batch, then we recommend delaying the opening of the remaining eggs for at least 1 additional day.

If poor viability or engraftment are obtained, several steps could be at fault. First, the embryo viability from the supplier may be poor. Absence of an air cell and visible vasculature indicates a nonviable egg. Sometimes, embryo movement can be visualized to confirm viability. First, though, ensure that fresh batteries are in the egg candler, because a strong light is needed for visualization. The float test may also be done to assess viability (a variety of instructions and videos are available online). Another possible explanation for poor viability is the incubator. Using an independent hygrometer and thermometer, ensure that the settings are accurate and stable. Manufacturer's instructions for the incubator should contain detailed troubleshooting instructions to assess proper settings. Improper incubator settings could also compromise CAM development. Using tape and/or a marker, determine if the egg rotator is actually spinning the eggs. If nonstick rings sink into the albumin in a high proportion of the engrafted eggs, then the CAM did not adequately develop. Finally, we have found that frequent checking of the engrafted egg, leading to temperature and humidity fluctuations, may decrease postimplant viability. If implanted eggs are initially viable, but the viability decreases throughout the engraftment period, the eggs should be checked less frequently. This decrease in viability could also be due to inaccurate or inappropriate incubator settings after implantation.

When optimizing this method for a new cell type, several factors can be controlled. The first is cell number. We typically implant 5×10^5-2×10^6 cells from cell lines. Implanted tumor pieces are typically 2–5 mm on each side. These amounts may be adjusted to improve engraftment or size. However, we have found that tumor growth lessens above a certain threshold, which is cell type dependent. Additional engraftment parameters include the presence or absence of a nonstick ring. This choice is typically made based on whether the ring will hinder the endpoint analysis, although it may also influence successful engraftment. The presence of the nonstick ring may also permit covering the nascent graft with medium at desired intervals to improve survival prior to vascular recruitment, if so desired. The choice of extracellular matrix type, concentration, and medium in which the matrix is diluted may also impact engraftment. The addition of growth factors or hormones may further improve tumor take rate or size. The selection of additives and concentrations would need to be done based on what would be appropriate for the specific cell type and not interfere with the experiment. These would also have the potential to be replenished at intervals if a nonstick ring is used.

Future applications of this model system depend on the hypothesis to be tested. For example, these tumor grafts could be used to test novel therapeutic approaches to reduce tumor size or deplete a subpopulation of the tumor. Co-implantation with cells from the host tumor microenvironment could permit studies of the influence of these cells on a variety of parameters, including tumor growth and treatment resistance. This model could also serve as an opportunity to incrementally expand primary human tumors prior to establishing xenografts in immunocompromised animal models. The initial adaptation to CAM

engraftment could perhaps facilitate tumor take rate in murine models. These applications have yet to be tested, but warrant further exploration.

Acknowledgments

The authors wish to thank Dr. Fuyuhiko Tamanoi and Binh Vu for the initial training on this method. Discussions with Dr. Eva Koziolek have been instrumental in optimizing this approach and have been very much appreciated. This work would not have been possible without funding from the following sources: the Tobacco-Related Disease Research Program Postdoctoral Fellowship (27FT-0023, to ACS), the Department of Defense (DoD) Ovarian Cancer Research Program (W81XWH-17-1-0160), NCI/NIH (1R21CA216770), Tobacco-Related Disease Research Program High Impact Pilot Award (27IR-0016), and UCLA institutional support, including a JCCC Seed Grant (NCI/NIH P30CA016042) and a 3R Grant from Office of the Vice Chancellor for Research to LW.

References

1. Kersten K, de Visser KE, van Miltenburg MH, Jonkers J Genetically engineered mouse models in oncology research and cancer medicine. EMBO Molecular Medicine. 9 (2), 137–153 (2017). [PubMed: 28028012]
2. Jackson SJ, Thomas GJ Human tissue models in cancer research: looking beyond the mouse. Disease Models & Mechanisms. 10 (8), 939–942 (2017). [PubMed: 28768734]
3. Cheon D-J, Orsulic S Mouse Models of Cancer. Annual Review of Pathology: Mechanisms of Disease. 6 (1), 95–119 (2011).
4. Howlader N et al. SEER Cancer Statistics Review, 1975–2016. National Cancer Institute Bethesda, MD, https://seer.cancer.gov/csr/1975_2016/ based on November 2018 SEER data submission, posted to the SEER web site, 4 (2019).
5. Ribatti D Chicken chorioallantoic membrane angiogenesis model. Methods Molecular Biology. 843 47–57 (2012).
6. Nowak-Sliwinska P, Segura T, Iruela-Arispe ML The chicken chorioallantoic membrane model in biology, medicine and bioengineering. Angiogenesis. 17 (4), 779–804 (2014). [PubMed: 25138280]
7. Lokman NA, Elder AS, Ricciardelli C, Oehler MK Chick chorioallantoic membrane (CAM) assay as an in vivo model to study the effect of newly identified molecules on ovarian cancer invasion and metastasis. International Journal of Molecular Science. 13 (8), 9959–9970 (2012).
8. Xiao X et al. Chick Chorioallantoic Membrane Assay: A 3D Animal Model for Study of Human Nasopharyngeal Carcinoma. PLoS ONE. 10 (6), e0130935 (2015). [PubMed: 26107941]
9. Deryugina EI, Quigley JP Chick embryo chorioallantoic membrane model systems to study and visualize human tumor cell metastasis. Histochemistry and Cell Biology. 130 (6), 1119–1130 (2008). [PubMed: 19005674]
10. Shoin K et al. Chick Embryo Assay as Chemosensitivity Test for Malignant Glioma. Japanese Journal of Cancer Research. 82 (10), 1165–1170 (1991). [PubMed: 1955382]
11. Hagedorn M et al. Accessing key steps of human tumor progression in vivo by using an avian embryo model. Proceedings of the National Academy of Science U S A. 102 (5), 1643–1648 (2005).
12. Kavaliauskaitė D et al. The Effect of Sodium Valproate on the Glioblastoma U87 Cell Line Tumor Development on the Chicken Embryo Chorioallantoic Membrane and on EZH2 and p53 Expression. BioMed Research International. 2017, 12 (2017).
13. Liu M et al. The Histone Methyltransferase EZH2 Mediates Tumor Progression on the Chick Chorioallantoic Membrane Assay, a Novel Model of Head and Neck Squamous Cell Carcinoma. Translational Oncology. 6 (3), 273–281 (2013). [PubMed: 23730406]
14. Rudy SF et al. In vivo Wnt pathway inhibition of human squamous cell carcinoma growth and metastasis in the chick chorioallantoic model. Journal of Otolaryngology - Head & Neck Surgery. 45 (1), 26 (2016). [PubMed: 27117272]
15. Canale S et al. Interleukin-27 inhibits pediatric B-acute lymphoblastic leukemia cell spreading in a preclinical model. Leukemia. 25, 1815 (2011). [PubMed: 21701492]

16. Loos C et al. Amino-functionalized nanoparticles as inhibitors of mTOR and inducers of cell cycle arrest in leukemia cells. Biomaterials. 35 (6), 1944–1953 (2014). [PubMed: 24331713]
17. Rovithi M et al. Development of bioluminescent chick chorioallantoic membrane (CAM) models for primary pancreatic cancer cells: a platform for drug testing. Scientific Reports. 7, 44686 (2017). [PubMed: 28304379]
18. Majerník M, et al. Novel Insights into the Effect of Hyperforin and Photodynamic Therapy with Hypericin on Chosen Angiogenic Factors in Colorectal Micro-Tumors Created on Chorioallantoic Membrane. International Journal of Molecular Science. 20 (12), 3004 (2019).
19. Swadi R et al. Optimising the chick chorioallantoic membrane xenograft model of neuroblastoma for drug delivery. BMC Cancer. 18 (1), 28 (2018). [PubMed: 29301505]
20. Klingenberg M, Becker J, Eberth S, Kube D, Wilting J The chick chorioallantoic membrane as an in vivo xenograft model for Burkitt lymphoma. BMC Cancer. 14 (1), 339 (2014). [PubMed: 24884418]
21. Avram S et al. Standardization of A375 human melanoma models on chicken embryo chorioallantoic membrane and Balb/c nude mice. Oncology Reports. 38 (1), 89–99 (2017). [PubMed: 28535001]
22. Zabielska-Koczywas K et al. 3D chick embryo chorioallantoic membrane model as an in vivo model to study morphological and histopathological features of feline fibrosarcomas. BMC Veterinary Research. 13 (1), 201 (2017). [PubMed: 28651614]
23. Skowron MA et al. Applying the chicken embryo chorioallantoic membrane assay to study treatment approaches in urothelial carcinoma. Urologic Oncology: Seminars and Original Investigations. 35 (9), 544.e511–544.e523 (2017).
24. Jefferies B et al. Non-invasive imaging of engineered human tumors in the living chicken embryo. Scientific Reports. 7 (1), 4991 (2017). [PubMed: 28694510]
25. Taizi M, Deutsch VR, Leitner A, Ohana A, Goldstein RS A novel and rapid in vivo system for testing therapeutics on human leukemias. Experimental Hematology. 34 (12), 1698–1708 (2006). [PubMed: 17157167]
26. Strojnik T, Kavalar R, Barone TA, Plunkett RJ Experimental model and immunohistochemical comparison of U87 human glioblastoma cell xenografts on the chicken chorioallantoic membrane and in rat brains. Anticancer Research. 30 (12), 4851–4860 (2010). [PubMed: 21187462]
27. Ribatti D The chick embryo chorioallantoic membrane as a model for tumor biology. Experimental Cell Research. 328 (2), 314–324 (2014). [PubMed: 24972385]
28. Hu J et al. A Non-integrating Lentiviral Approach Overcomes Cas9-Induced Immune Rejection to Establish an Immunocompetent Metastatic Renal Cancer Model. Molecular Therapy - Methods & Clinical Development. 9, 203–210 (2018). [PubMed: 29766028]

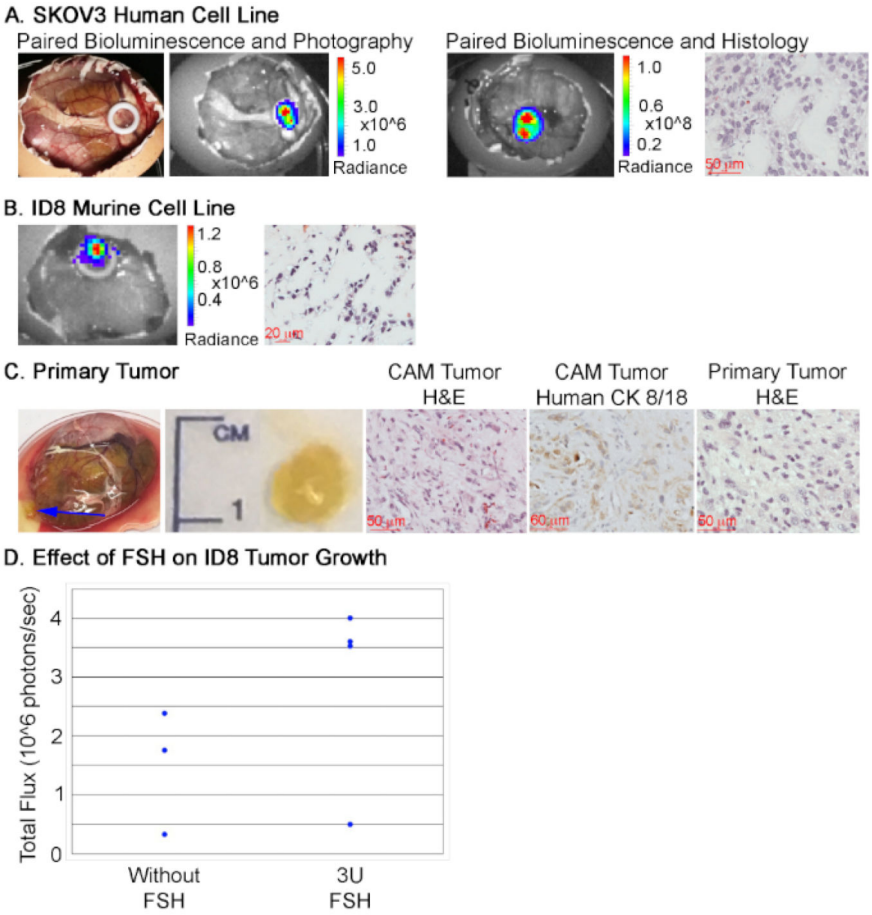

Figure 1: Representative tumor development from ovarian cancer.

Ovarian cancer cells successfully implanted include: (**A**) the human SKOV3 cell line, (**B**) the murine ID8 cell line, and (**C**) primary tumors. Representative hematoxylin and eosin staining is presented along with bioluminescence imaging, as appropriate. For the CAM tumor resulting from the implantation of a primary tumor piece (**C**) hematoxylin and eosin staining of both the CAM tumor and primary tumor are included, along with cytokeratin 8/18 (CK 8/18) staining of the resulting CAM tumor. The blue arrow in the first panel indicates the tumor. (**D**) Tumor size of ID8 implants with and without 3U FSH, calculated as the total flux resulting from bioluminescence imaging (n = 3 for untreated and n = 4 for FSH-supplemented).

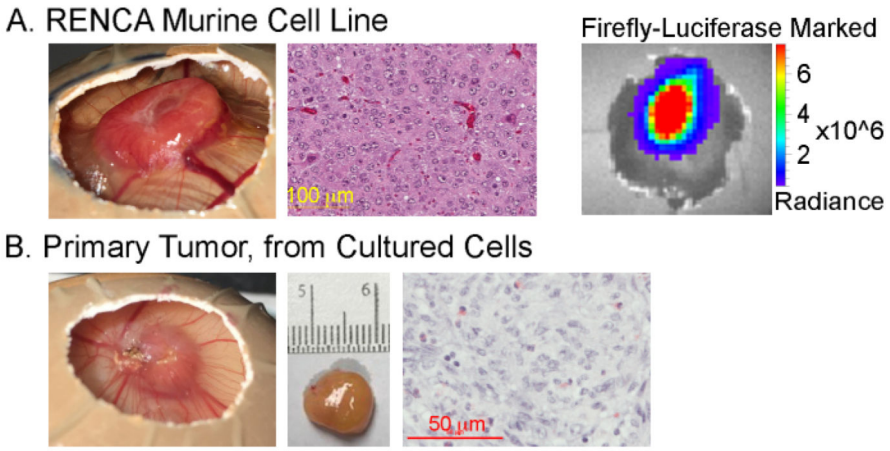

Figure 2: Representative tumor development from clear cell renal cell carcinoma.

Tumors resulting from implantation of (**A**) the murine renal cell carcinoma cell line, RENCA, or (**B**) cultured cells derived from a digested human primary tumor. The measurement scale adjacent to the excised tumor in (**B**) shows 1 mm markings. Corresponding histology in (**A**) and (**B**) shows hematoxylin and eosin staining. In (**A**), the representative bioluminescence imaging of firefly-luciferase-marked RENCA cells is also shown.

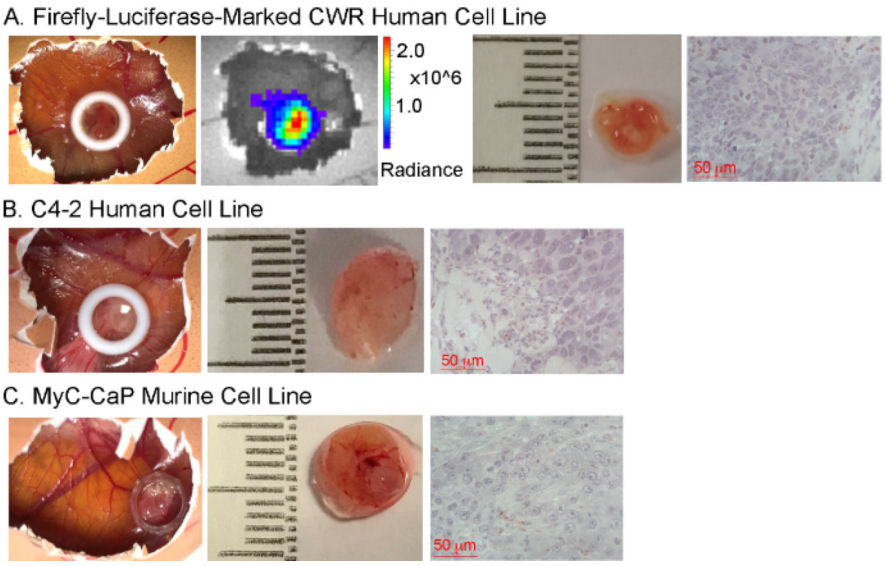

Figure 3: Representative tumor development from prostate cancer cell lines.

Representative tumors and hematoxylin and eosin staining resulting from the implantation of the human prostate cancer cell lines (**A**) CWR and (**B**) C4–2 along with the murine cell line (**C**) MyC-CaP. Bioluminescence imaging of the resulting tumors from firefly luciferase marked CWR cells is shown in (**A**). The measurement scale adjacent to the excised tumors shows 1 mm markings.

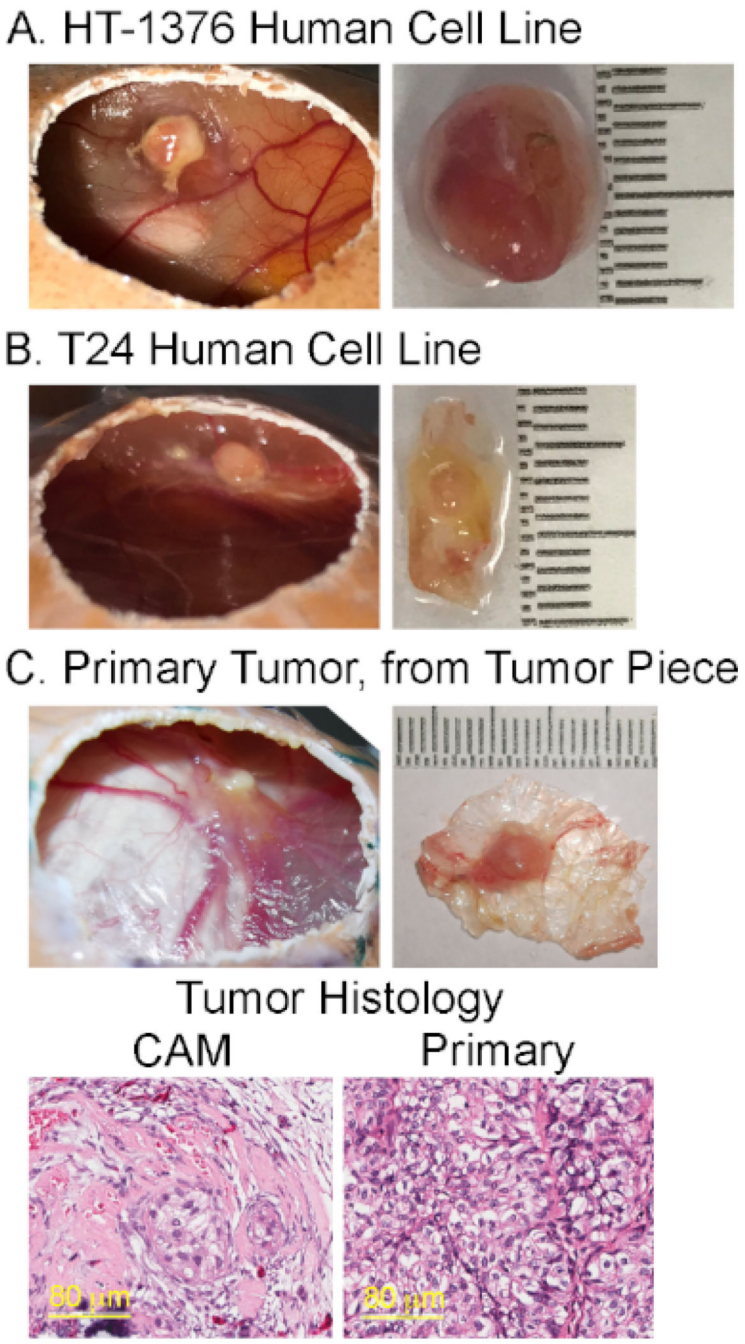

Figure 4: Representative tumor development from bladder cancer.

Representative tumors resulting from the implantation of the established human bladder cancer cell lines (**A**) HT-1376, (**B**) T24, and (**C**) primary human bladder tumor. In (**C**), hematoxylin and eosin staining of the resulting CAM tumor and the primary tumor are shown. The measurement scale adjacent to the excised tumors shows 1 mm markings.